

Effect of lead and zinc composition on the optical and structural characteristics of PbZnS thin films fabricated by spray pyrolysis

S. Çelik ^{a,*}, M. Temiz ^b

^a *Engineering of Physics Department, Gaziantep University, 27200 Gaziantep/Turkey*

^b *University of Selcuk Karapınar Aydoğanlar Vocational School, 42400 Konya/Turkey*

In this study, PbZnS thin films with varying concentrations of lead (Pb) and zinc (Zn) were successfully produced using the spray pyrolysis method. The structural, optical and surface properties of the films were systematically investigated as a function of the Pb/Zn ratio. X-ray diffraction (XRD) analysis confirmed the polycrystalline nature of the films, showing a cubic zinc blende structure with improved crystallinity as Pb content increased. Initially, with the increase in Pb concentration, larger crystallite sizes and decreased microstress were observed, but with the increase of Pb addition, the formation of secondary phases and the emergence of lattice distortions caused a decrease in grain size and an increase in microstress. Optical measurements showed a tunable bandgap in the range of 3.25 eV to 1.30 eV as Pb content increased. The narrowing of the bandgap is attributed to the lower energy gap of PbS compared to ZnS, which allows for enhanced absorption of longer-wavelength light, especially in the visible and near-infrared regions. These findings highlight the potential of PbZnS thin films for optoelectronic applications, where the ability to tune the bandgap and enhance absorption through compositional adjustments is crucial for optimizing device performance. The surface morphology of the PbZnS thin films was analyzed using scanning electron microscopy (SEM). The SEM images showed notable changes in grain size and surface roughness as Pb content increased, with larger grains and a more distinct surface structure observed in films with higher Pb concentrations. This work demonstrates the versatility of spray pyrolysis in fabricating thin films with controllable properties, offering valuable insights for future applications in energy conversion technologies, including solar cells and photodetectors.

(Received October 10, 2024; Accepted January 23, 2025)

Keywords: PbZnS thin films, Structural properties, Optical properties, Spray pyrolysis, Band gap energy

1. Introduction

Thin films play a very important role in modern optoelectronic devices, especially in photovoltaic applications, sensors and other semiconductor-based technologies. Metal chalcogenides such as lead and zinc sulfide have drawn considerable attention among thin film materials owing to their modifiable optical and structural characteristics. PbZnS, a ternary compound, offers a unique combination of properties by varying the ratio of its elements (lead (Pb) and zinc (Zn)) in its structure. This makes it a promising candidate for advanced technological applications.

Compared to many other thin film coating procedures, spray pyrolysis method, which is a relatively simple and cost-effective method, stands out as a usable method for the production of such thin films. This method allows users to make precise adjustments to the film composition, morphology and thickness. Thanks to these adjustments, it becomes easy to examine the impacts of compositional changes on material properties. Since the changing metal concentrations of films produced with spray pyrolysis technique significantly change the optical absorption, band gap

* Corresponding author: ssur@gantep.edu.tr
<https://doi.org/10.15251/CL.2025.221.89>

energy and crystallinity of the material, the interest in studies related to this subject has grown considerably in the past few years.

In addition to optical and structural analysis, surface morphology plays a critical role in the material's functionality. The SEM images of the PbZnS thin films reveal the impact of varying Pb and Zn concentrations on grain size and surface roughness, which are key indicators of film quality and performance

In this research, we investigated the optical, structural and surface properties of PbZnS thin films growth using spray pyrolysis. We systematically varied the Pb and Zn content in the films, aiming to understand how these compositional changes affect the fundamental material features. The focus of our study is to determine to what extent the Pb/Zn ratio affects parameters such as crystallite size, surface morphology, and optical band gap, which are critical for tailoring the material for specific optoelectronic applications. This study adds to the expanding knowledge base regarding metal chalcogenide thin films and provides insights into optimizing PbZnS films for practical applications in energy conversion and other related fields.

2. Experimental studies

2.1. Materials and preparation

PbZnS thin films were produced by employing the spray pyrolysis technique onto glass substrates. Precursor solutions were prepared by dissolving lead acetate ($\text{Pb}(\text{CH}_3\text{CO}_2)_2 \cdot 3\text{H}_2\text{O}$), zinc acetate ($\text{Zn}(\text{CH}_3\text{CO}_2)_2 \cdot 2\text{H}_2\text{O}$) and thiourea ($\text{CH}_4\text{N}_2\text{S}$) in deionized water in appropriate amounts according to the calculated ratios for each sample. To adjust the film compositions, varying amounts of Pb and Zn were added to the solution and mixed. The stoichiometric ratio of sulfur (S) in the PbZnS compound was not supposed to change, so the thiourea concentration was kept constant. The molar concentrations of Pb and Zn were varied because it was desired to research the impacts of Pb and Zn on the structural and optical features of the films. The substrates were subjected to a cleaning process before deposition to remove any contamination and ensure good adhesion on the films. Acetone, ethanol and deionized water were used for the cleaning process. The films were cleaned ultrasonically and then air dried.

2.2. Spray pyrolysis deposition

The spray pyrolysis system is a simple but very practical system consisting of parts such as a nozzle, a precursor solution container and a heated substrate holder. Compressed air was used to atomize the prepared precursor solutions. Glass substrates were heated to approximately 350°C and the prepared solution was sprayed onto these substrates. Homogeneous and consistent film thickness contributes significantly to the physical features of the thin films[1], therefore, the solution flow rate and spraying time were carefully controlled to obtain homogeneous and consistent film thicknesses. During the deposition process, great importance was given to ensuring that the physical environment conditions and experimental set settings were the same, and the distance between the nozzle and the substrate was maintained as 20 cm.

3. Results and discussion

3.1. Structural properties

Figure 1 demonstrates the X-ray diffraction (XRD) patterns of PbZnS thin films produced at different levels of Pb and Zn concentrations. All the films we fabricated showed distinct diffraction peaks corresponding to the polycrystalline structure of PbZnS.

The interplanar spacing (d) is calculated with the equations given below.

$$2d\sin\Theta = n\lambda \quad (1)$$

where Θ is the Bragg angle and λ is the wavelength of X-ray.

Using the equation given above, the lattice parameter for the cubic phase is calculated as follows[2].

$$a = d_{hkl}\sqrt{h^2 + k^2 + l^2} \quad (2)$$

We calculated the lattice parameters for the films grown at different base temperatures using the corresponding formula and plotted them in figure 1.

The Scherrer formula we use to determine the crystal grain size (t) of films is given as follows[3]:

$$t = \frac{0,9\lambda}{\beta \cos\theta} \quad (3)$$

where β , λ , and θ are the full width at half maximum (FWHM) of the peak, the 1.5406 Å wavelength of the X-ray, and their peak position, respectively.

The microstrain (ϵ) in the films produced with varying amounts of Pb and Zn was derived from the following formula [4]:

$$\rho = \frac{15\epsilon}{aD} \quad (4)$$

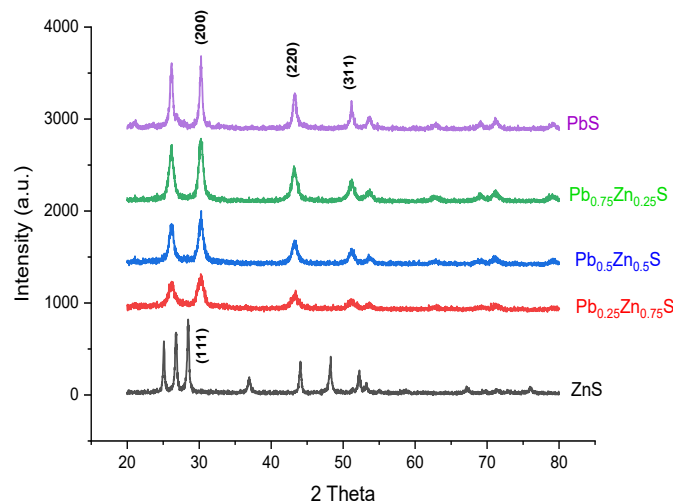


Fig. 1. X-ray diffraction (XRD) patterns of PbZnS thin films produced via the spray pyrolysis method with varying Pb and Zn concentrations.

Increasing Pb content makes the prominent diffraction peaks corresponding to the (111), (220) and (311) planes of the cubic zinc blende structure become more pronounced. With the increase in Pb concentrations, an increase in peak intensities and a decrease in peak widths are observed, indicating improved crystallinity and larger crystallite sizes.

Table 1. The 2θ values, distance between planes, lattice constant, grain size and micro strain of PbZnS films with varying Pb and Zn concentrations.

	2 Θ Value ($^{\circ}$)	Inter- Planner d (A°)	Lattice Constant A°	Grain size (nm)	Microstrain
ZnS	28,46	3,1338	5,4279	25,4815	0,0136019
Pb _{0,25} Zn _{0,75} S	30,12	2,9649	5,1353	32,2422	0,0119948
Pb _{0,5} Zn _{0,5} S	30,25	2,9524	5,1137	43,4751	0,0108754
Pb _{0,75} Zn _{0,25} S	30,14	2,9632	5,1325	21,3587	0,0162270
PbS	30,10	2,9666	5,1383	15,7456	0,0911866

When we analyze figure 1 and table 1 in detail, we observe that with the rising in Pb content and the declining in Zn content, the crystal lattice expands and the grain size increases. This is because Pb has a larger ionic radius compared to Zn. Since there will be fewer defects in larger and more shaped grains, a decrease in microstress occurs[5].

However, while this increase continues, we observe that after a certain Pb concentration, this situation reverses. When too much Pb is added to the structure, some defects and secondary phases that disrupt grain growth begin to appear, resulting in a decrease in grain size. In addition, the inclusion of excessive amounts of Pb atoms in the lattice can create lattice distortions and increase microstrain. Moreover, the decrease in Zn, which is critical for stabilizing the ZnS phase, can also contribute to this distortion of the crystal structure, further increase microstrain, and lead to the emergence of smaller, strained grains[6, 7].

This behavior shows us that there is a delicate balance between Pb and Zn in the system, where the optimum ratio promotes crystal growth, while too much Pb causes structural integrity to deteriorate.

3.2. Optical properties

UV-Vis spectroscopy was utilized to study the optical characteristics of PbZnS thin films. The absorbance profiles of the films grown with varying Pb and Zn concentrations are shown in Fig. 2. All films exhibited significant absorption in the 400-1800 nm range, with a notable shift in the absorption edge as the Pb content increased. This shift indicates changes in the optical bandgap of the films as the Pb/Zn ratio was altered.

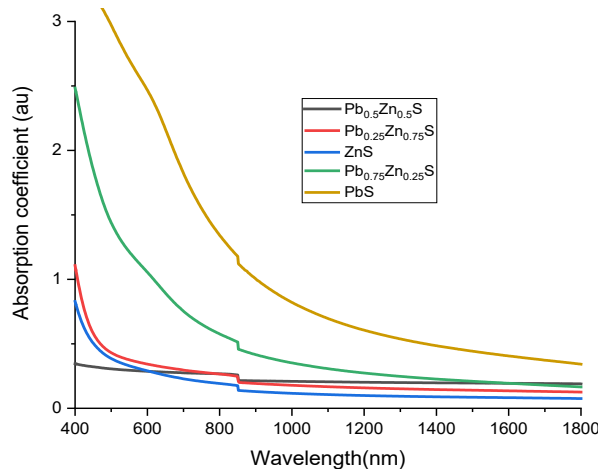


Fig. 2. Absorption spectra of the PbZnS thin films with different Pb and Zn concentrations.

The optical bandgap (E_g) figures for the films were calculated based on the relationship between the absorption coefficient (α) and the photon energy ($h\nu$), which can be expressed as follows[8]:

$$(\alpha h\nu) = A(h\nu - E_g)^{1/2} \quad (5)$$

where A is defined as a coefficient connected to the effective masses. The band gap values are calculated from plots of $(\alpha h\nu)^2$ against $h\nu$ by extrapolating the linear portion of the line to the energy axis at $\alpha = 0$ (Figure 3). The bandgap values ranged from 3,25 eV to 1,30 eV as the Pb content increased. Initially, with a higher Zn concentration, the films exhibited a wider bandgap, characteristic of ZnS, which has a bandgap of approximately 3.6 eV. As Pb was introduced and its concentration increased, the bandgap narrowed, reflecting the lower bandgap of PbS, around 0.41 eV[9]. This tunability of the bandgap with varying Pb and Zn concentrations is a critical feature for applications in optoelectronics. The narrowing bandgap with increasing Pb content allows the films

to absorb light more effectively in the visible range, making them suitable for applications such as photodetectors and solar cells. The ability to adjust the bandgap through compositional control highlights the versatility of PbZnS thin films for use in various energy-related technologies[10].

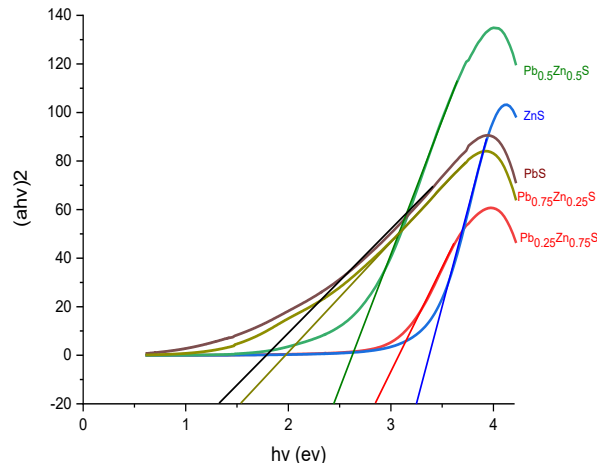


Fig. 3. Plots of $(ahv)^2$ vs. $h\nu$ of the PbZnS thin films with different Pb and Zn concentrations.

As the Pb content increases and Zn decreases in PbZnS films, we would generally expect the absorption coefficient to increase. This behavior can be ascribed to various factors associated with the material properties of PbS and ZnS.

Narrower Bandgap of PbS: PbS has a much lower bandgap (~ 0.41 eV) compared to ZnS (~ 3.6 eV). When the Zn content is reduced and more Pb is incorporated, the overall bandgap of the film decreases. A smaller bandgap allows the material to absorb lower-energy photons (longer wavelengths), leading to enhanced absorption in the visible and near-infrared regions of the spectrum[11].

Higher Density of States in PbS: PbS typically has a higher density of states near the conduction and valence bands relative to ZnS. This means that more electronic transitions can occur at specific photon energies, contributing to an increase in the absorption coefficient as more Pb is added[12].

Optical Transitions in PbS: PbS is known for its strong optical absorption due to direct optical transitions. As Pb content increases, these transitions become more dominant, enhancing the absorption over a broader spectral range, particularly in the infrared region where ZnS is less effective[13].

3.3. Surface morphology analysis of PbZnS thin films

In order to better understand the surface morphology and microstructural characteristics of the PbZnS thin films, scanning electron microscopy (SEM) was employed. The SEM images provide valuable insight into the grain distribution, surface roughness, and the effect of varying Pb and Zn concentrations on the film structure.

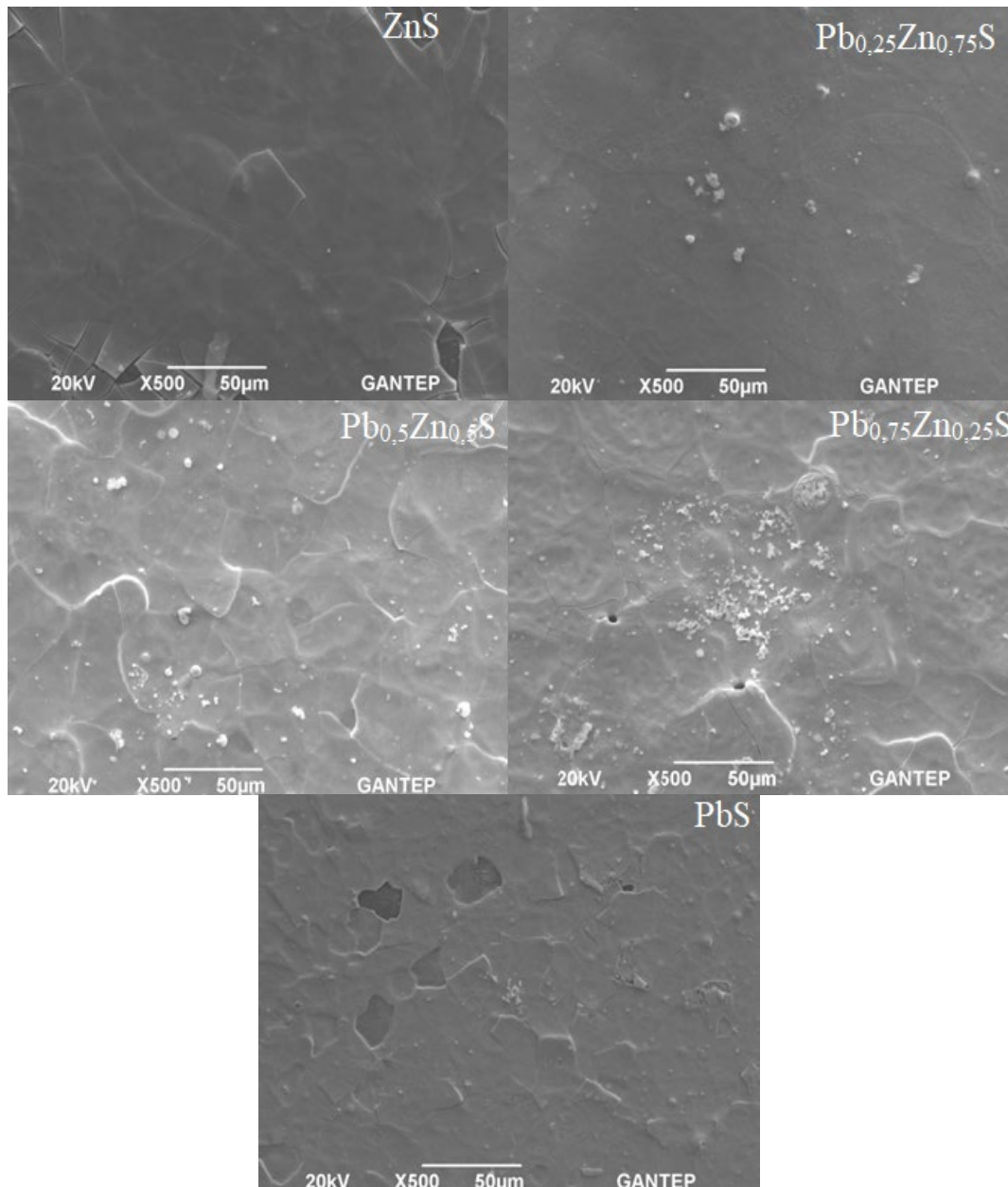


Fig. 4. SEM images of PbZnS thin films fabricated using the spray pyrolysis method with varying Pb and Zn concentrations.

The images reveal significant changes in the surface morphology as the Pb content increases. At lower Pb concentrations, the films exhibit a relatively uniform and compact grain structure, while higher Pb concentrations lead to larger, more distinct grains with visible surface roughness. These morphological changes align with the XRD results, where increasing Pb content initially promotes grain growth but later introduces defects and secondary phases that hinder further crystallization[14].

4. Conclusions

In this study, PbZnS thin films with varying Pb and Zn compositions were successfully synthesized using the spray pyrolysis method. Structural analysis revealed that the films exhibit a polycrystalline cubic zinc blende structure, with the crystallinity improving as the Pb content

increased. XRD results indicated that an increase in Pb concentration led to higher peak intensities and narrower peak widths, reflecting improved crystallinity and larger grain sizes. However, when Pb content exceeded a critical value, grain growth was inhibited, likely due to the formation of secondary phases and lattice distortions, resulting in a reduction in grain size and increased microstrain.

Optical analysis demonstrated that the bandgap of the PbZnS films could be tuned by altering the Pb/Zn ratio. As Pb content increased, the bandgap narrowed significantly, shifting from ~ 3.25 eV to ~ 1.30 eV. This bandgap reduction, along with enhanced absorption in the visible and near-infrared regions, is attributed to the dominance of PbS, which has a much lower bandgap than ZnS. The higher density of states and direct optical transitions in PbS further contributed to increased absorption with higher Pb content.

The examination of surface morphology through SEM imaging has further illuminated the relationship between Pb and Zn concentrations and their effects on film characteristics. The observed grain size and surface roughness variations underscore the importance of optimizing elemental ratios to enhance the structural and optical properties of PbZnS thin films for potential applications in optoelectronic devices.

These results suggest that by controlling the Pb/Zn ratio, the optical and structural properties of PbZnS films can be tailored, making them suitable for applications in optoelectronic devices, such as photodetectors and solar cells, where tunable bandgaps and enhanced absorption are critical. This research adds valuable insights into optimizing the compositional design of metal chalcogenide thin films for energy-related applications.

References

- [1] Hind A, Chomette L (2003) The determination of thin film thickness using reflectance spectroscopy. Agil Technol Inc 1-4
- [2] Cullity BD (Bernard D (1978) Elements of x-ray diffraction. Addison-Wesley Publishing Company, Inc
- [3] Birks LS, Friedman H (1946), J Appl Phys 17:687-692; <https://doi.org/10.1063/1.1707771>
- [4] Temiz M (2021) Investigation of Structural, Optical and Electrical Properties of Undoped and Boron Doped Indium Oxide Films Growth by Spray Pyrolysis Technique. Gaziantep University
- [5] 8.2: Atomic and Ionic Radius - Chemistry LibreTexts. https://chem.libretexts.org/Courses/Bellarmine_University/BU%3A_Chem_103_%28Christianston%29/Phase_3%3A_Atoms_and_Molecules_-_the_Underlying_Reality/8%3A_Periodic_Trends_in_Elements_and_Compounds/8.2%3A_Atomic_and_Ionic_Radius. Accessed 4 Oct 2024
- [6] Zhao Y, Zhang J (2008), J Appl Crystallogr 41:1095-1108; <https://doi.org/10.1107/S0021889808031762>
- [7] Attaf A, Derbali A, Saidi H, et al (2020), Phys Lett A 384:126199; <https://doi.org/10.1016/j.physleta.2019.126199>
- [8] Ravishankar S, Balu AR, Anbarasi M, Nagarethinam VS (2015), Optik (Stuttg) 126:2550-2555; <https://doi.org/10.1016/j.ijleo.2015.06.039>
- [9] Liu M, Zhan Q, Li W, et al (2019), J Alloys Compd 792:1000-1007; <https://doi.org/10.1016/j.jallcom.2019.04.117>
- [10] Suhail M (2020) Structural and optical properties of ZnS , PbS , Zn_{1-x}Pb_xS , Zn_xPb_{1-x}S and PbZn_xS_{1-x} thin films Structural and optical properties of ZnS, PbS , Zn_{1-x}Pb_xS , Zn_xPb_{1-x}S and PbZn_xS_{1-x} thin films
- [11] Vamvasakis I, Andreou EK, Armatas GS (2023), Nanomaterials 13:2426; <https://doi.org/10.3390/nano13172426>
- [12] Lany S, Zunger A (2007), Phys Rev Lett 98: <https://doi.org/10.1103/PhysRevLett.98.045501>

[13] Bernard JE, Zunger A (1987), Phys Rev B 36:3199;
<https://doi.org/10.1103/PhysRevB.36.3199>

[14] Huo J, Li W, Wang T (2019), Coatings 2019, Vol 9, Page 376 9:376;
<https://doi.org/10.3390/coatings9060376>